PROCEEDINGS OF SCIENCE

Lambda Hypernuclear Spectroscopy by Electron Scattering at JLab

Toshiyuki Gogami,[a,*] **Franco Garibaldi,**[b,c] **Pete Markowitz,**[d] **Joerg Reinhold,**[d] **Sho Nagao,**[e] **Satoshi N. Nakamura,**[e,f] **Liguang Tang**[g,h] **and Guido Urciuoli**[b]

[a] *Department of Physics, Graduate School of Science, Kyoto University, Kyoto 606-8502, Japan*
[b] *INFN, Sezione di Roma, 00185 Rome, Italy*
[c] *Istituto Superiore di Sanità, 00161 Rome, Italy*
[d] *Department of Physics, Florida International University, Miami, FL 33199, USA*
[e] *Graduate School of Science, The University of Tokyo, Tokyo 113-0033, Japan*
[f] *Quark Nuclear Science Institute, Graduate School of Science, The University of Tokyo, Tokyo 113-0033, Japan*
[g] *Department of Physics, Hampton University, Hampton, VA 23668, USA*
[h] *Thomas Jefferson National Accelerator Facility (JLab), Newport News, VA 23606, USA*

E-mail: gogami.toshiyuki.4a@kyoto-u.ac.jp

Hypernuclei are good tools to investigate hyperon-nucleon and hyperon-hyperon interactions. Missing-mass spectroscopy of Λ hypernuclei with the $(e, e'K^+)$ reaction, which was established at Jefferson Laboratory (JLab), is able to achieve high resolution and high accuracy. In the next experimental campaign at JLab's Experimental Hall C starting from 2027, we will measure Λ hypernuclei with a wide mass range from light to heavy systems ($^{6}_{\Lambda}$He, $^{9}_{\Lambda}$Li, $^{11}_{\Lambda}$Be, $^{27}_{\Lambda}$Mg, $^{40}_{\Lambda}$K, $^{48}_{\Lambda}$K, and $^{208}_{\Lambda}$Tl) by using high-resolution spectrometers, HES and HKS. The systematic investigations would provide us new information on ΛN charge symmetry breaking, nuclear deformations, ΛNN three-body interaction, and so on.

The XVIth Quark Confinement and the Hadron Spectrum Conference (QCHSC24)
19-24 August, 2024
Cairns Convention Centre, Cairns, Queensland, Australia

*Speaker

 ISSN 1824-8039 . Published by SISSA Medialab.

PoS(QCHSC24)230

1. Introduction

Hypernuclei are important tools to investigate the strong interactions between hyperon and nucleon (YN) and/or between hyperon and hyperon (YY). A straightforward way to investigate the strong interaction is the scattering experiment which has been used for nucleon-nucleon (NN) interaction studies. However, data of the scattering experiments for the YN and YY systems are limited due to experimental difficulties originating from short lifetimes of hyperons while modern experiments successfully observed YN scattering events at Japan Proton Accelerator Research Complex, Japan (J-PARC) [1–3] and Jefferson Laboratory, US (JLab) [4]. Femtoscopy, which measures correlation functions of particles in heavy-ion collision experiments gives insights into the strong interactions between hadrons. For example, the interactions of Ξ-p and Λ-Λ were found to be weakly attractive by comparing the data obtained at CERN [5–7] with the calculations based on the YN/YY interactions simulated by lattice QCD [8]. The femtoscopy provides the information of spin-averaged baryon interactions. Similarly, the experimental difficulties of the scattering experiments with hyperons, particularly for the preparation of polarized hyperons, have been preventing us from using the scattering experiment for investigating the spin-dependent interactions, although a new idea of polarized hyperon scattering experiment at J-PARC is being discussed [9]. The hypernuclear masses and production-cross sections contain rich information on the strong interactions including the spin-dependent interactions. In this article, we describe missing-mass spectroscopy of Λ hypernuclei by electron scattering at JLab.

2. Missing-Mass Spectroscopy with the $(e, e'K^+)$ Reaction

Typical reactions for the missing-mass spectroscopy of Λ hypernuclei are the (K^-, π^-), (π^+, K^+), and $(e, e'K^+)$ reactions. The (K^-, π^-) and (π^+, K^+) reactions use hadron beams which are provided as secondary beams. On the other hand, $(e, e'K^+)$ uses a primary electron beam. Therefore, the quality of incident particles such as the energy spread and the emittance is better for the $(e, e'K^+)$ reaction than the (K^-, π^-) and (π^+, K^+) reactions. If the energy spread and drift are small enough, and the energy central is well determined for the primary beam, one does not need to measure momentum vectors of the beam event by event for a missing-mass measurement. This allows us not to install any tracking devices combined with a spectrometer used for the angle and momentum analyses of incident particles. A typical rate capability of tracking devices is on the order of 10^6–10^7 charged particles per second (cpps). Indeed, the beam intensity of the hadron beams such as π^+ and K^- is limited to 10^6–10^7 cpps due to the rate capability of detectors. In the case of the use of primary electron beams, on the other hand, much higher intensity is available and usable for the missing-mass measurement because of no use of particle detectors for the beam particles. A typical beam intensity of the JLab's electron beam is 10–100 μA which corresponds to the order of $I_e = 10^{13}$–10^{14} per second. The high intensity of the electron beam is essential for hypernuclear measurement because of the smaller cross section of the $(e, e'K^+)$ reaction than those of the other reactions. The $(e, e'K^+)$ reaction may be treated as the (γ^*, K^+) reaction as a virtual photon mediates in the $(e, e'K^+)$ reaction [10, 11]. The hypernuclear production-cross section of the (γ^*, K^+) reaction is about 10 nb/sr which is smaller by two to three orders of magnitude than that of the (π^+, K^+) reaction. One has to be noted that the virtual photon flux needs to be taken into

account. The virtual photon flux Γ is determined by the detection acceptance of scattered electrons. The virtual photon flux is $\Gamma \sim 10^{-5}$ per electron if High resolution scattered Electron Spectrometer (HES) [12] is assumed. It means that $(1/\Gamma =)10^5$ electrons would make a virtual-photon beam for the reaction. The intensity of the virtual photon is calculated by multiplying Γ by the beam intensity, $I_{\gamma^*} = \Gamma \times I_e = 10^9$–$10^{10}$ per second. The virtual photon intensity is larger by three to four orders of magnitude than the hadron beams, which compensates the smaller cross section. In addition, even thinner targets would yield enough number of hypernuclear signals due to the high beam intensity, given a limited beam time. A typical areal density of an experimental target is 0.1 g/cm^2 for the $(e, e'K^+)$ reaction while it is 1–10 g/cm^2 for the (π^+, K^+) and (K^-, π^-) reactions. A thinner target leads to a smaller effect of the energy straggling of incident and scattered particles in the target material, which is actually one of the important factors to reach both high resolution and high accuracy in the Λ hypernuclear spectroscopy with the $(e, e'K^+)$ reaction. For example, the achieved energy resolutions in the missing-mass spectra were 0.5 and 1.45 MeV in FWHM for the $(e, e'K^+)$ and (π^+, K^+) reactions, respectively [13, 14].

The $(e, e'K^+)$ reaction converts a proton into a Λ while the (K^-, π^-) and (π^+, K^+) reactions convert a neutron into a Λ. The proton conversion allows us to use a proton target at rest such as polyethylene (CH_2) and hydrogen-gas targets etc. for producing hyperons. On the other hand, one cannot use a neutron target at rest because the lightest atom which contains a neutron is deuterium in which the neutron in the nucleus has the Fermi momentum. The hyperon productions from the proton target at rest are observed as peaks with a finite width due to only the experimental resolution. In JLab E05-115 experiment, which is Λ hypernuclear spectroscopy with the $(e, e'K^+)$ reaction at JLab's Hall C performed in 2009 [12, 13], successfully observed sharp peaks of both Λ and Σ^0 productions with the resolution of 1.5 MeV/c^2 in FWHM as shown in Fig. 1. The events of hyperon

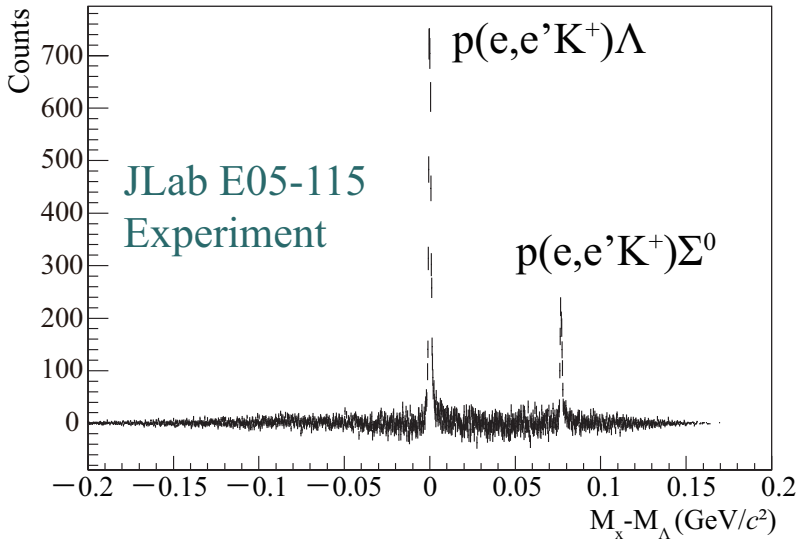

Figure 1: Λ and Σ^0 production events observed in JLab E05-115 Experiment which used the $p(e, e'K^+)$X reaction with the polyethylene target (CH_2) [12]. The horizontal axis is the reconstructed missing mass subtracted by the mass of Λ (M_Λ). The background events due to accidental coincidence and carbon nuclei were subtracted in the spectrum. The events of the hyperon productions were used for the energy scale calibration.

productions were used for the energy calibration as the masses of Λ and Σ^0 are well known. The systematic error on the binding energy measurement was $\Delta B_\Lambda^{\rm sys.} = 0.11$ MeV thanks to the good calibration data acquired with the same experimental condition of the hypernuclear data [12]. The difference of the nucleon to be converted into the Λ is an important feature in terms of expanding the nuclear chart with the strangeness degree of freedom. In addition, mirror hypernuclei are produced if one selects proper experimental targets. For example, $A = 10$ iso-doublet hypernuclei, ${}^{10}_{\Lambda}$B and ${}^{10}_{\Lambda}$Be, are produced from a ^{10}B target with the (π^+, K^+) and $(e, e'K^+)$ reactions, respectively. Comparisons of the Λ binding energies of mirror hypernuclei allow us to investigate the charge symmetry breaking in the ΛN interaction (ΛN CSB).

3. Overview of the Next Hypernuclear Experiments at JLab

Hypernuclear experiments approved by the Program Advisory Committee (PAC) of JLab [15–20] are listed in Tab. 1. The experiments, except for E12-19-002, are planned to be performed with a common experimental setup. The E12-19-002 experiment needs cryogenic gas targets of H_2 and ^{3,4}He, and a vertical bending spectrometer for the production-vertex analysis as required in the previous hypernuclear experiment with the tritium-gas target at JLab's Hall A [21–24]. On the other hand, the other experiments use only solid targets which require a much simpler development of the target system. In addition, there is no need to use the vertical bending spectrometer, which means existing spectrometers developed for hypernuclear spectroscopy (HES and HKS) [12, 25, 26] can be used without any major modifications. Therefore, we decided to carry out the experimental projects that use the solid targets for the next run, and the experiments with the gaseous targets afterward. The run group experiment E12-15-008A was endorsed in JLab PAC in 2024. The other experiments measure the momentum vectors of e' and K^+ by using the magnetic spectrometers, HES and HKS, for reconstructing the masses of Λ hypernuclei (missing-mass spectroscopy). On the other hand, the E12-15-008A experiment uses an additional spectrometer, ENGE, installed at a backward angle to detect π^- from the two-body weak decay of Λ hypernuclei (decay-pion spectroscopy). It is noted that ENGE is a split-pole spectrometer [27] that was used for the e' detection in the past hypernuclear spectroscopy at JLab [28, 29]. Some of the produced hypernuclei may decay with the two-body processes at rest in the target, and emit π^-'s with specific momenta determined by the masses of parent hypernuclei. In other words, the π^- momentum tells us the mass of Λ hypernucleus. A feasibility of the decay-pion spectroscopy was proven at MAMI, Germany, where the Λ binding energy of the ground state of ${}^{4}_{\Lambda}$H was determined with high accuracy by using a ^{9}Be target [30, 31]. At MAMI, recently, the decay pion spectroscopy was performed with a ^{7}Li target to determine the ground state binding energy of ${}^{3}_{\Lambda}$H with the accuracy of a few 10 keV [35–37]. The data analysis is in progress. The decay-pion spectroscopy at JLab, which will be kept running during the missing-mass spectroscopy, will acquire more statistics from various experimental targets. Thus, the ground state energies of various Λ hypernuclei particularly for light nuclear systems are expected to be determined with the accuracy of a few 10 keV by the decay-pion spectroscopy.

3.1 Study of ΛN Charge Symmetry Breaking

One of the important features of the ΛN interaction is the charge symmetry breaking (ΛN CSB). ΛN CSB was found in the binding energy difference of $A = 4$ iso-doublet hypernuclei, ${}^{4}_{\Lambda}$H and ${}^{4}_{\Lambda}$He.

Table 1: Hypernuclear experiments approved and endorsed by JLab PAC [15–20]. The experiments, except for JLab E12-19-002, are planned to be performed with a common experimental setup at JLab Hall C, and are scheduled to be started in 2027.

Experiment	Hypernucleus	Title	PAC Days
E12-19-002	${}^{3}_{\Lambda}$H, ${}^{4}_{\Lambda}$H	High accuracy measurement of nuclear masses of hyperhydrogens	14.5
E12-24-004	${}^{6}_{\Lambda}$He, ${}^{9}_{\Lambda}$Li, ${}^{11}_{\Lambda}$Be	Study of charge symmetry breaking in p-shell hypernuclei	24
E12-24-013	${}^{40}_{\Lambda}$K, ${}^{48}_{\Lambda}$K	An isospin dependence of the ΛN interaction through the high precision spectroscopy of Lambda hypernuclei	55
E12-24-011	${}^{27}_{\Lambda}$Mg	Study of a triaxially deformed nucleus using a Lambda particle as a probe	28
E12-24-003	${}^{208}_{\Lambda}$Tl	Studying Lambda interactions in nuclear matter with the ^{208}Pb$(e,e'K^+)^{208}_{\Lambda}$Tl reaction	42
Run group (E12-15-008A)		High-resolution spectroscopy of light hypernuclei with the decay-pion spectroscopy	N/A

The energy difference of the ground state was found to be $\Delta B_\Lambda({}^{4}_{\Lambda}\mathrm{He}-{}^{4}_{\Lambda}\mathrm{H};J^\pi=0^+)=+350\pm40$ keV in nuclear emulsion experiments [38–40], and later the difference was updated to be $+233\pm92$ keV by the decay-pion spectroscopy of ${}^{4}_{\Lambda}$H at MAMI [30, 31]. The large difference in energy is attributed to ΛN CSB because the Coulomb correction does not cancel out the difference and even makes the difference larger by 20–50 keV [32–34]. On the other hand, there is no energy difference in the first excited states (1^+); $\Delta B_\Lambda({}^{4}_{\Lambda}\mathrm{He}-{}^{4}_{\Lambda}\mathrm{H};1^+)=-0.083\pm0.094$ MeV [41]. Therefore, ΛN CSB depends on the spin. To pin down the origin of ΛN CSB, the investigation was extended to p-shell Λ hypernuclei. The binding energy comparison for the $A=7$ iso-triplet hypernuclei, ${}^{7}_{\Lambda}$He, ${}^{7}_{\Lambda}$Li* and ${}^{7}_{\Lambda}$Be, is one of the examples [42]. The Λ binding energies of ${}^{7}_{\Lambda}$Li* and ${}^{7}_{\Lambda}$Be were obtained by the emulsion experiment [38] and γ-ray spectroscopy [43]. On the other hand, the energy of ${}^{7}_{\Lambda}$He measured by the emulsion experiment has a broadened distribution, and thus, the energy was not precisely determined [44–46]. Two independent experiments, JLab E01-011 and E05-115, which are missing-mass spectroscopy experiments by the $(e,e'K^+)$ reaction at JLab, successfully obtained the ${}^{7}_{\Lambda}$He energy, $B_\Lambda^{\text{E01-011}}({}^{7}_{\Lambda}\mathrm{He};1/2^+)=5.68\pm0.03^{\text{stat.}}\pm0.25^{\text{sys.}}$ MeV [47] and $B_\Lambda^{\text{E05-115}}({}^{7}_{\Lambda}\mathrm{He};1/2^+)=5.55\pm0.10^{\text{stat.}}\pm0.11^{\text{sys.}}$ MeV [48], respectively. The weighted average is $B_\Lambda({}^{7}_{\Lambda}\mathrm{He};1/2^+)=5.58\pm0.13$ MeV when a square root of the quadratic sum of statistical and systematic errors is taken into account as a total error for each result. The experimental data were compared with the theoretical calculation by the cluster model with the phenomenological CSB potential [42]. Parameters of the phenomenological CSB potential were adjusted to reproduce existing data of ${}^{4}_{\Lambda}$H, ${}^{4}_{\Lambda}$He, ${}^{8}_{\Lambda}$Li, and ${}^{8}_{\Lambda}$Be. It turned out that the calculation without the phenomenological CSB potential has a better consistency with the data [48], and one may need a more sophisticated treatment such as

a consideration of ΛN-ΣN coupling [49–51]. The discussion in the $A = 7$ iso-triplet system further stimulated the ΛN CSB study in p-shell systems as discussed in Ref. [52]. Theoretical calculations of binding energy differences for some p-shell iso-multiplet hypernuclei were performed [42, 53–55]. However, the uncertainties of the existing experimental data are too large to clarify the validity of the theoretical models. Therefore, energy measurements as accurate as 100 keV or less are awaited, and high accuracy measurements are planned at JLab as well as J-PARC [56, 57]. JLab E12-24-004 will measure the missing-mass spectra for $^{6}\mathrm{Li}(e,e'K^+)^{6}_{\Lambda}\mathrm{He}$, $^{9}\mathrm{Be}(e,e'K^+)^{9}_{\Lambda}\mathrm{Li}$, and $^{11}\mathrm{B}(e,e'K^+)^{11}_{\Lambda}\mathrm{Be}$. In addition, JLab E12-19-002 will measure the $^{3}\mathrm{He}(e,e'K^+)^{3}_{\Lambda}\mathrm{H}$ and $^{4}\mathrm{He}(e,e'K^+)^{4}_{\Lambda}\mathrm{H}$ reactions [58]. It is worth noting that JLab E12-15-008A (decay-pion spectroscopy) is expected to provide ground state energies of various light Λ hypernuclei.

3.2 Study of Nuclear Deformation by using Λ as Probe

The nuclear density distribution of a core nucleus in Λ hypernucleus affects the Λ binding energy because of a change of the wavefunction overlap between the core nucleus and Λ [59–62]. Hypernuclear states with a Λ residing in the p-orbit (p_Λ) coupled with the α-α structure of ^{8}Be in parallel with and perpendicular to the axis of two α's were observed as independent states in the missing-mass spectrum of $^{9}\mathrm{Be}(\pi^+,K^+)^{9}_{\Lambda}\mathrm{Be}$ [63, 64]. A similar argument has been made in theoretical analyses of the observed spectrum of $^{10}\mathrm{B}(e,e'K^+)^{10}_{\Lambda}\mathrm{Be}$ at JLab [65] by using the distorted wave-impulse approximation with the shell-model framework that considers excited states of unnatural parity states as well as natural parity states of the core nucleus [66–68]. In the $^{9}\mathrm{Be}(e,e'K^+)^{9}_{\Lambda}\mathrm{Li}$ spectrum, a deformed structure in the 3^+ state of ^{8}Li was indicated by observing the smaller Λ binding energy of the third doublet peak ($5/2^+_2, 7/2^+$; $\mathrm{Li}^{8}(3^+)\otimes s_\Lambda$) than that of shell-model predictions [69]. As shown above, the Λ hyperon behaves as a probe to investigate nuclear density distributions. We are trying to observe the triaxially deformed states in ^{26}Mg by the high resolution spectroscopy of $^{27}_{\Lambda}$Mg in JLab E12-24-011. The deformation property of the ^{26}Mg nucleus is not known well because $N = 14$ and $Z = 12$ favor different shapes in the Nilsson diagram [70]. Λ binding energies of $^{27}_{\Lambda}$Mg in the p_Λ state coupled with the triaxially deformed states of ^{26}Mg are expected to be split into three doublet states by about 2 MeV from each other as predicted for the case of $^{25}_{\Lambda}$Mg [71]. Therefore, the observation of such a phenomenon needs an experimental resolution as good as 1 MeV or better. JLab E12-24-011, which is the spectroscopy of $^{27}\mathrm{Al}(e,e'K^+)^{27}_{\Lambda}\mathrm{Mg}$ with the missing-mass resolution of 0.6 MeV in FWHM, would give us new insights into the triaxial deformation states.

3.3 Study of ΛNN Three Body Force

The presence of hyperons such as Λ in neutron stars reduces the predicted maximum mass of the neutron stars because of the softening of the equation of state (EOS). The softening of the EOS prevents neutron stars from reaching the observed large masses, such as $1.97(4)M_\odot$ [72] and $2.01(4)M_\odot$ [73]. The three-body ΛNN interaction may play an important role in theoretically supporting the existence of the large mass neutron stars [74–77]. The three-body ΛNN interaction is predicted to have a larger effect on the binding energy of Λ hypernucleus as the mass number gets larger [78, 79]. Therefore, the precise and accurate measurements of $^{40}\mathrm{Ca}(e,e'K^+)^{40}_{\Lambda}\mathrm{K}$, $^{48}\mathrm{Ca}(e,e'K^+)^{48}_{\Lambda}\mathrm{K}$ (JLab E12-24-013) and $^{208}\mathrm{Pb}(e,e'K^+)^{208}_{\Lambda}\mathrm{Tl}$ (JLab E12-24-003) are expected to give us new information on the ΛNN interaction. In addition, the isospin dependence of the

ΛN interaction would be important for the study of neutron stars because the composition of neutron stars is dominated by neutrons. The precise comparison of energy spectra of ${}^{40}_{\Lambda}$K and ${}^{48}_{\Lambda}$K through careful analyses which consider both the predicted production-cross sections and the energy structures [11, 80] would reveal a hint for the isospin dependence of the ΛN interaction [81, 82].

3.4 Apparatus and Preparation Status of the New Experiments

We describe the apparatus used for missing-mass spectroscopy in this article. Figure 2 shows the experimental setup for the next hypernuclear experiments at JLab Hall C. The electron beam at $E_e = 2.24$ GeV is incident on the experimental target, and the scattered electron (e') and K^+ are measured by HES and HKS, respectively. The central momentum of HES is set to 0.74 GeV/c to utilize the virtual photon at the energy of $\omega = 1.5$ GeV where the production cross sections of Λ and Σ^0 are large. The central momentum of HKS is 1.2 GeV/c to detect hypernuclear production as well as the productions of Λ and Σ^0 under the same experimental conditions. A Pair of Charge Separation dipole magnets (PCS) is installed at the front of the HES-HKS system for guiding e' and K^+ toward opposite directions. PCS is composed of two separate dipole magnets so that there is no strong magnetic field along the beamline. The feature of no strong magnetic field along the beamline avoids the contamination of e^+ into HKS, and thus leads to a better signal-to-noise ratio than the previous hypernuclear experiment, JLab E05-115 [12]. Transportation of PCS to JLab has been completed, followed by the construction in Japan. A Monte-Carlo simulation based on Geant4 was performed to estimate the momentum resolutions of (PCS+) HES and (PCS+) HKS. As a result, the resolutions are estimated to be $\Delta p/p = 4.4 \times 10^{-4}$ and $\Delta p/p = 2.9 \times 10^{-4}$ in FWHM for HES and HKS, respectively. Based on the simulation, the estimated missing-mass resolution and accuracy are 0.6 MeV/c^2 (FWHM) and $\Delta B_{\Lambda}^{\rm total} = 0.07$ MeV, respectively. The basic parameters of the experiments are summarized in Tab. 2. The momenta and angles of e' and K^+ at the target are reconstructed by using backward transfer matrices (BTMs). Sieve slits that are made of tungsten alloy are installed at the entrance of PCS. The matrix elements for the angle reconstruction are optimized to realize the sieve-slit patterns. On the other hand, the matrix elements for the momentum reconstruction are optimized by using the data of the $p(e, e'K^+)\Lambda$ and $p(e, e'K^+)\Sigma^0$ reactions from a polyethylene target. The BTM analysis and the parameter optimization, which corresponds to the energy calibration, were established in the previous hypernuclear experiments at JLab. For more information of the calibration, see Refs. [12, 21, 83].

HES has a honeycomb-cell multi-wire drift chamber (EDC) for the particle tracking, and time-of-flight (TOF) counters (ETOF1–2) for the data-taking trigger and TOF measurement. On the other hand, HKS has planar multi-wire drift chambers (KDC1–2), TOF counters (TOF1X, 1Y, 2X), and two types of Cherenkov counters (WC1–2, AC1–3) for the particle identification. All detectors, except for WC, are existing and now they are being commissioned by tests with cosmic rays at JLab. We are preparing the new water Cherenkov detector (WC) because reflection materials attached to the inner surface of the old WC were partially unstuck. Water tanks of WC will be shipped to JLab in 2025 after the mass production in Japan. We are also preparing other components such as data acquisition system, analysis software, target system, beam-diagnosis system, etc. aiming for being ready for the experiments by 2027.

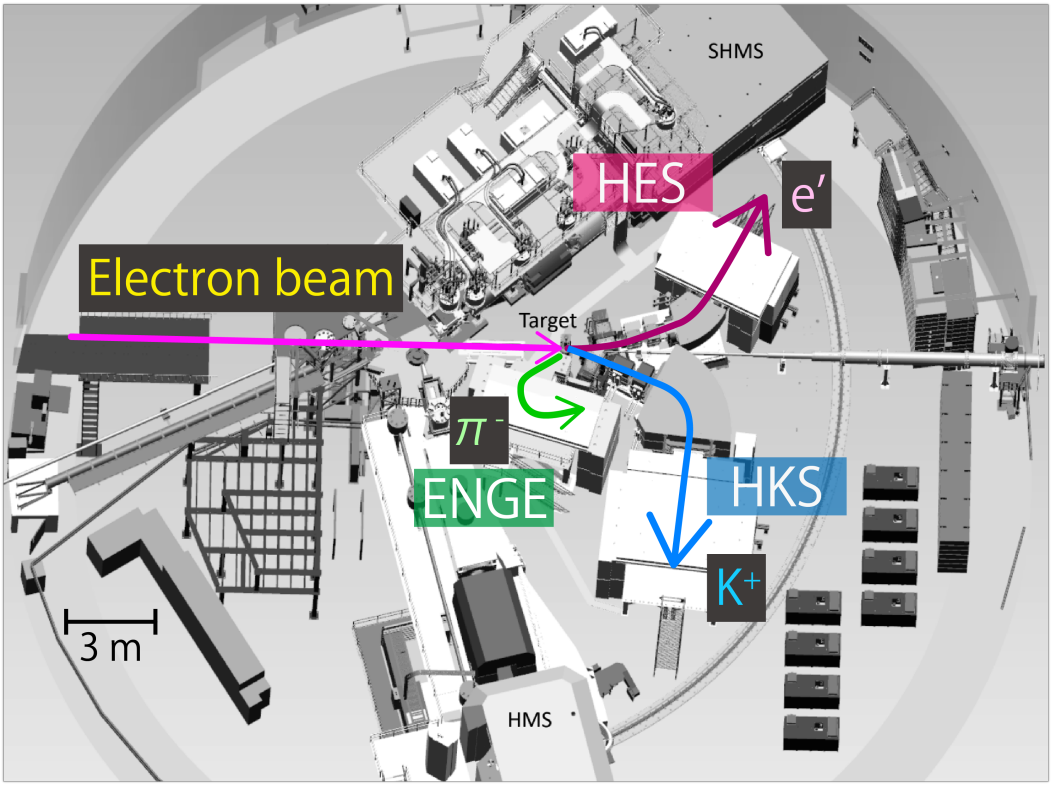

Figure 2: Experimental setup for the next hypernuclear experiments at JLab Hall C. HES and HKS measure momentum vectors of e' and K^+ at the target. The mass of Λ hypernucleus (missing mass) is calculated once the momentum vectors of e^+ and K^+ are reconstructed because the energy and angle of the primary electron beam is well controlled and determined. ENGE is used for decay-pion spectroscopy of Λ hypernuclei.

Table 2: Basic parameters of the next hypernuclear experiments at JLab Hall C.

Item		Value
Beam (e)	Energy (/GeV)	2.24
	(Required) energy spread and drift	1×10^{-4} (FWHM)
PCS + HES (e')	Central momentum $p^{\text{cent.}}_{e'}$ [/(GeV/c)]	0.74
	Central angle $\theta^{\text{cent.}}_{ee'}$	8.5°
	Solid angle acceptance $\Omega_{e'}$ (/msr) (at $p^{\text{cent.}}_{e'}$)	3.4
	Momentum resolution $\Delta p_{e'}/p_{e'}$	4.4×10^{-4} (FWHM)
PCS + HKS (K^+)	Central momentum $p^{\text{cent.}}_{K^+}$ [/(GeV/c)]	1.20
	Central angle $\theta^{\text{cent.}}_{eK^+}$	11.5°
	Solid angle acceptance Ω_{K^+} (/msr) (at $p^{\text{cent.}}_{K^+}$)	7.0
	Momentum resolution $\Delta p_{K^+}/p_{K^+}$	2.9×10^{-4} (FWHM)
$p(e,e'K^+)\Lambda$	$\sqrt{s} = W$ (/GeV)	1.912
	Q^2 [/(GeV/c)^2]	0.036
	K^+ scattering angle wrt virtual photon, $\theta_{\gamma^* K^+}$	7.35°
	ϵ	0.59
	ϵ_L	0.0096

4. Summary

Λ hypernuclear spectroscopy from light to heavy mass region ($^{6}_{\Lambda}$He, $^{9}_{\Lambda}$Li, $^{11}_{\Lambda}$Be, $^{27}_{\Lambda}$Mg, $^{40}_{\Lambda}$K, $^{48}_{\Lambda}$K, and $^{208}_{\Lambda}$Tl) is scheduled to be performed at JLab's Experimental Hall C from 2027. High-resolution spectrometers, HES and HKS, combined with new magnets (PCS) will be used for missing-mass spectroscopy with the $(e, e'K^+)$ reaction. The expected missing-mass resolution and energy accuracy are 0.6 MeV/c^2 in FWHM and $\Delta B_{\Lambda}^{\rm total}$ = 0.07 MeV, respectively. In addition, decay-pion spectroscopy of various light Λ hypernuclei will be kept being performed during the missing-mass spectroscopy by using the additional spectrometer, ENGE. The comprehensive experimental campaign would provide new insights into ΛN charge symmetry breaking, nuclear deformations, ΛNN three-body interaction, and so on.

Acknowledgments

This work was partially supported by the Grant-in-Aid for Scientific Research on Innovative Areas "Toward new frontiers Encounter and synergy of state-of-the-art astronomical detectors and exotic quantum beams." This work was supported by JSPS KAKENHI grants nos. 24H00219, 24K00657, 23H00114, 22KK0040, 18H05459, 18H05457, 18H01219, and 17H01121. This work was also supported by SPIRITS 2020 of Kyoto University, and the Graduate Program on Physics for the Universe, Tohoku University (GP-PU).

References

[1] K. Miwa *et al.*, *Measurement of the differential cross sections of the $\Sigma^- p$ elastic scattering in momentum range 470 to 850 MeV/c*, *Phys. Rev. C* **104**, 045204 (2021).

[2] K. Miwa *et al.*, *Precise measurement of differential cross section of the $\Sigma^- p \to \Lambda n$ reaction in momentum range 470–650 MeV/c*, *Phys. Rev. Lett.* **128**, 072501 (2022).

[3] T. Nanamura *et al.*, *Measurement of differential cross section for $\Sigma^+ p$ elastic scattering in the momentum range 0.44–0.80 GeV/c*, *Prog. Theor. Exp. Phys.* **2022**, 9, 093D01 (2022).

[4] J. W. Price, *Λp elastic scattering in the CLAS detector*, *AIP Conf. Proc.* **2130**, 020004 (2019).

[5] S. Acharya *et al.*, *Study of the Λ-Λ interaction with femtoscopy correlations in pp and p-Pb collisions at the LHC*, *Phys. Lett. B* **797**, 134822 (2019).

[6] S. Acharya *et al.*, *First observation of an attractive interaction between a proton and a cascade baryon*, *Phys. Rev. Lett.* **123**, 112002 (2019).

[7] S. Acharya *et al.*, *Unveiling the strong interaction among hadrons at the LHC*, *Nature* **588**, 232 (2020).

[8] Y. Kamiya *et al.*, *Femtoscopic study of couples channels $N\Xi$ and $\Lambda\Lambda$ interactions*, *Phys. Rev. C* **105**, 014915 (2022).

[9] T. Sakao *et al.*, *Λ polarization measurement of the $\pi^- p \to K^0\Lambda$ reaction in J-PARC E40 experiment*, *EPJ Web Conf.* **271**, 02008 (2022).

[10] T. Motoba, M. Sotona, K. Itonaga, *Photoproduction of polarized hypernuclei*, *Prog. Theor. Phys. Suppl.* **117**, 123–133 (1994).

[11] T. Motoba, P. Bydžovský, M. Sotona, K. Itonaga, *Spectroscopy of electro- and photo-productions of hypernuclei*, *Prog. Theor. Phys. Suppl.* **185**, 224–251 (2010).

[12] T. Gogami *et al.*, *Experimental techniques and performance of Λ-hypernuclear spectroscopy with the $(e, e'K^+)$ reaction*, *Nucl. Instrum. Methods Phys. A* **900**, 69–83 (2018).

[13] L. Tang *et al.*, *Experiments with the high resolution kaon spectrometer at JLab Hall C and the new spectroscopy of ${}^{12}_{\Lambda}$B hypernuclei*, *Phys. Rev. C* **90**, 034320 (2014).

[14] H. Hotchi *et al.*, *Spectroscopy of medium-heavy Λ hypernuclei via the (π^+, K^+) reaction*, *Phys. Rev. C* **64**, 044302 (2001).

[15] T. Gogami, F. Garibaldi, P. Markowitz, S. N. Nakamura, J. Reinhold, L. Tang, G. M. Urciuoli, *High Accuracy Measurement of Nuclear Masses of Λ Hyperhydrogens*, *Proposal to JLab PAC* **49**, JLab E12-19-002 (2021).

[16] T. Gogami, F. Garibaldi, P. Markowitz, S. Nagao, S. N. Nakamura, J. Reinhold, L. Tang, G. M. Urciuoli, *Study of Charge Symmetry Breaking in P-shell Hypernuclei*, *Proposal to JLab PAC* **52**, JLab E12-24-004 (2024).

[17] S. N. Nakamura, F. Garibaldi, T. Gogami, P. Markowitz, S. Nagao, J. Reinhold, L. Tang, G. M. Urciuoli, *An isospin dependence of the ΛN interaction through the high precision spectroscopy of Lambda hypernuclei*, *Proposal to JLab PAC* **52**, JLab E12-24-013 (2024); update from JLab E12-15-008.

[18] S. N. Nakamura, F. Garibaldi, T. Gogami, P. Markowitz, S. Nagao, J. Reinhold, L. Tang, G. M. Urciuoli, *Study of a triaxially deformed nucleus using a Lambda particle as a probe*, *Proposal to JLab PAC* **52**, JLab E12-24-011 (2024).

[19] F. Garibaldi, T. Gogami, P. Markowitz, S. Nagao, S. N. Nakamura, J. Reinhold, L. Tang, G. M. Urciuoli, *Studying Lambda interactions in nuclear matter with the ^{208}Pb$(e, e'K^+)^{208}_{\Lambda}$Tl reaction*, *Proposal to JLab PAC* **52**, JLab E12-24-003 (2024); update from JLab E12-20-013.

[20] S. Nagao, F. Garibaldi, T. Gogami, P. Markowitz, S. N. Nakamura, J. Reinhold, L. Tang, G. M. Urciuoli, *High-resolution spectroscopy of light hypernuclei with the decay-pion spectroscopy*, *Run group addition endorsed by JLab PAC* **52**, JLab E12-20-013A/E12-15-008A (2024).

[21] K. N. Suzuki *et al.*, *The cross-section measurement for the ^{3}H$(e, e'K^+)nn\Lambda$ reaction*, *Prog. Theor. Exp. Phys.* **2022**, 1, 013D01 (2022).

[22] B. Pandey *et al.*, *Spectroscopic study of a possible Λnn resonance and a pair of ΣNN states using the $(e, e'K^+)$ reaction with a tritium target*, *Phys. Rev. C* **105**, L051001 (2022).

[23] T. Gogami *et al.*, *Cross-section measurement of virtual photoproduction of iso-triplet three-body hypernucleus, Λnn*, *EPJ Web Conf.* **271**, 02002 (2022).

[24] K. Okuyama *et al.*, *Electroproduction of the Λ/Σ^0 hyperons at $Q^2 \simeq 0.5$ $(\mathrm{GeV}/c)^2$ at forward angles*, *Phys. Rev. C* **110**, 025203 (2024).

[25] T. Gogami *et al.*, *Bucking coil implementation on PMT for active canceling of magnetic field*, *Nucl. Instrum. Methods Phys. A* **729**, 816–824 (2013).

[26] Y. Fujii *et al.*, *High-precision three-dimensional field maping of a high resolution magnetic spectrometer for hypernuclear spectroscopy at JLab*, *Nucl. Instrum. Methods Phys. A* **795**, 351–363 (2015).

[27] H. A. Enge, *Magnetic spectrographs for nuclear reaction studies*,*Nucl. Instrum. Methods* **162**, 161–180 (1979).

[28] T. Miyoshi *et al.*, *High resolution spectroscopy of the ${}^{12}_{\Lambda}\mathrm{B}$ hypernucleus produced by the $(e, e'K^+)$ reaction*, *Phys. Rev. Lett.* **90**, 232502 (2003).

[29] L. Yuan *et al.*, *Hypernuclear spectroscopy using the $(e, e'K^+)$ reaction*, *Phys. Rev. C* **73**, 044607 (2006).

[30] A. Esser *et al.*, *Observation of ${}^{4}_{\Lambda}\mathrm{H}$ hyperhydrogen by decay-pion spectroscopy in electron scattering*, *Phys. Rev. Lett.* **114**, 232501 (2015).

[31] F. Schulz *et al.*, *Ground-state binding energy of ${}^{4}_{\Lambda}\mathrm{H}$ from high-resolution decay pion spectroscopy*, *Nucl. Phys. A* **954**, 149 (2016).

[32] R. H. Dalitz, F. Von Hippel, *Electromagnetic Λ-Σ^0 mixing and charge symmetry for the Λ-hyperon*, *Phys. Lett.* **10**, 1, 153–157 (1964).

[33] J. L. Friar, B. F. Gibson, *Coulomb energies in S-shell nuclei and hypernuclei*, *Phys. Rev. C* **18**, 908 (1978).

[34] A. R. Bodmer, Q. N. Usmani, *Coulomb effects and charge symmetry breaking for the $A = 4$ hypernuclei*, *Phys. Rev. C* **31**, 1400 (1985).

[35] P. Eckert *et al.*, *Commissioning of the hypertriton binding energy measurement at MAMI*, *EPJ Web Conf.* **271**, 01006 (2022).

[36] P. Klag *et al.*, *High accuracy synchrotron radiation interferometry with relativistic electrons*, *J. Phys.: Conf. Ser.* **2482**, 012016 (2023).

[37] S. Nagao *et al.*, *High-resolution hypernuclear decay pion spectroscopy at MAMI and future*, *IL NUOVO CIMENTO* **47** C 232 (2024).

[38] M. Jurić *et al.*, *A new determination of the binding-energy values of the light hypernuclei ($A \leq 15$)*, *Nucl. Phys. B* **52**, 1 (1973).

[39] G. Bohm *et al.*, *On the lifetime of the* ${}^{3}_{\Lambda}$H *hypernucleus*, *Nucl. Phys. B* **4**, 511 (1968).

[40] D. H. Davis, *50 years of hypernuclear physics: I. The early experiments*, *Nucl. Phys. A* **754**, 3c–13c (2005).

[41] T. Yamamoto *et al.*, *Observation of spin-dependent charge symmetry breaking in ΛN interaction: gamma-ray spectroscopy of* ${}^{4}_{\Lambda}$He, *Phys. Rev. Lett.* **115**, 222501 (2015).

[42] E. Hiyama, Y. Yamamoto, T. Motoba, M. Kamimura, *Structure of A = 7 iso-triplet hypernuclei studied with the four-body cluster model*, *Phys. Rev. C* **80**, 054321 (2009).

[43] H. Tamura *et al.*, *Observation of a spin-flip M1 transition in* ${}^{7}_{\Lambda}$Li, *Phys. Rev. Lett.* **84**, 5963 (2000).

[44] J. Pniewski and M. Danysz, *A note on the* ${}^{7}_{\Lambda}$He *hyperfragments*, *Phys. Lett.* **1**, 142 (1962).

[45] R. H. Dalitz and A. Gal, *Isomeric states in* ${}^{7}_{\Lambda}$He, *Nucl. Phys. B* **1**, 1 (1967).

[46] J. Pniewski and Z. Szymański, D. H. Davis, and J. Sacton, *Is a* ${}^{7}_{\Lambda}$He *hyperisomer possible?*, *Nucl. Phys. B* **2**, 317 (1967).

[47] S. N. Nakamura *et al.*, *Observation of the* ${}^{7}_{\Lambda}$He *hypernucleus by the* $(e, e'K^{+})$ *reaction*, *Phys. Rev. Lett.* **110**, 012502 (2013).

[48] T. Gogami *et al.*, *Spectroscopy of the neutron-rich hypernucleus* ${}^{7}_{\Lambda}$He *from electron scattering*, *Phys. Rev. C* **94**, 021302(R) (2016).

[49] Y. Akaishi, T. Harada, S. Shinmura, K. Myint, *Coherent Λ-Σ coupling in s-shell hypernuclei*, *Phys. Rev. Lett.* **84**, 3539 (2000).

[50] A. Nogga, H. Kamada, and W. Glöckle, *The hypernuclei* ${}^{4}_{\Lambda}$He *and* ${}^{4}_{\Lambda}$H*: challenges for modern hyperon-nucleon forces*, *Phys. Rev. Lett.* **88**, 172501 (2002).

[51] D. Gazda and A. Gal, *Ab initio calculations of charge symmetry breaking in the A = 4 hypernuclei*, *Phys. Rev. Lett.* **116**, 122501 (2016).

[52] E. Botta, *Charge symmetry breaking in s- and p-shell Λ-hypernuclei: An update review*, *AIP Conf. Proc.* **2130**, 030003 (2019).

[53] E. Hiyama and Y. Yamamoto, *Structure of* ${}^{10}_{\Lambda}$Be *and* ${}^{10}_{\Lambda}$B *hypernuclei studied with the four-body cluster model*, *Prog. Theor. Phys.* **128**, 105 (2012).

[54] A. Gal and D. Gazda, *Charge symmetry breaking in light Λ hypernuclei*, *Jour. Phys.: Conf. Ser.* **966**, 012006 (2018).

[55] H. Le *et al.*, *Ab initio calculation of charge-symmetry breaking in A = 7 and 8 Λ hypernuclei*, *Phys. Rev. C* **107**, 24002 (2023).

[56] T. Gogami *et al.*, *Strangeness physics programs by S-2S at J-PARC*, *EPJ Web Conf.* **271**, 11002 (2022).

[57] T. Gogami *et al.*, *New generation Λ hypernuclear spectroscopy with the* (π^+, K^+) *reaction by S-2S*, *Proposal to the 34th J-PARC PAC*, J-PARC E94 Experiment (2022).

[58] T. Gogami *et al.*, *High accuracy spectroscopy of 3- and 4-body Λ hypernuclei at Jefferson Lab*, *EPJ Web Conf.* **271**, 01001 (2022).

[59] M. T. Win, K. Hagino, *Deformation of Λ hypernuclei*, *Phys. Rev. C* **78**, 054311 (2008).

[60] M. Isaka, K. Fukukawa, M. Kimura, E. Hiyama, H. Sagawa, Y. Yamamoto, *Superdeformed Λ hypernuclei with antisymmetrized molecular dynamics*, *Phys. Rev. C* **89**, 024310 (2014).

[61] M. Isaka, Y. Yamamoto, Th. A. Rijken, *Competing effects of nuclear deformation and density dependence of the ΛN interaction in* B_Λ *values of hypernuclei*, *Phys. Rev. C* **94**, 044310 (2016).

[62] H. T. Xue, Q. B. Chen, X. R. Zhou, Y. Y. Cheng, H. -J. Schulze, *Deformation and hyperon halo in hypernulei*, *Phys. Rev. C* **106**, 044306 (2022).

[63] H. Bando, K. Ikeda, T. Motoba, *Coupling features in* ${}^{9}_{\Lambda}$Be, ${}^{13}_{\Lambda}$C *and* ${}^{21}_{\Lambda}$Ne *hypernuclei*, *Prog. Theor. Phys.* **69**, 3, 918–928 (1983).

[64] O. Hashimoto, H. Tamura, *Spectroscopy of Λ hypernuclei*, *Prog. Par. Nucl. Phys.* **57**, 2, 564–653 (2006).

[65] T. Gogami *et al.*, *High resolution spectroscopic study of* ${}^{10}_{\Lambda}$Be, *Phys. Rev. C* **93**, 034314 (2016).

[66] T. Motoba, *Photoproduction of typical hypernuclei*, *JPS Conf. Proc.* **17**, 011003 (2017).

[67] A. Umeya, T. Motoba, K. Itonaga, *Structure and production cross section of p-shell Lambda-hypernuclei calculated with multi-configuration shell model*, *J. Phys.: Conf. Ser.* **1643**, 012110 (2020).

[68] A. Umeya, T. Motoba, K. Itonaga, *Hypernuclear production spectroscopy with an extended shell model*, *EPJ Web. Conf.* **271**, 01010 (2022).

[69] T. Gogami *et al.*, *Spectroscopy of* $A = 9$ *hyperlithium with the* $(e, e'K^+)$ *reaction*, *Phys. Rev. C* **103**, L041301 (2021).

[70] N. Hinohara and Y. Kanada, *Triaxial quadrupole deformation dynamics in sd-shell nuclei around* ^{26}Mg, *Phys. Rev. C* **83**, 014321 (2011).

[71] M. Isaka and M. Kimura, *Splitting of the p orbit in triaxially deformed* ${}^{25}_{\Lambda}$Mg, *Phys. Rev. C* **87**, 021304(R) (2013).

[72] P. B. Demorest *et al.*, *A two-solar-mass neutron star measured using Shapiro delay*, *Nature* **467**, 1081-1083 (2010).

[73] J. Antoniadis *et al.*, *A massive pulsar in a compact relativistic binary*, *Science* **340**, 1233232 (2013).

[74] D. Lonardoni, A. Lovato, S. Gandolfi, F. Pederiva, *Hyperon puzzle: Hints from quantum Monte Carlo Calculations*, *Phys. Rev. Lett.* **114**, 042301 (2015).

[75] D. Gerstung, N. Kaiser, W Wise, *Hyperon-nucleon three-body forces and strangeness in neutron stars*, *Eur. Phys. J. A* **56**, 175 (2020).

[76] A. Jinno, K. Murase, Y. Nara, A. Onishi, *Repulsive* Λ *potentials in dense neutron star matter and binding energy of* Λ *in hypernuclei*, *Phys. Rev. C* **108**, 065803 (2023).

[77] H. Le, J. Haidenbauer, U. G. Meißner, A. Nogga, *Light* Λ *hypernuclei studied with chiral hyperon-nucleon and hyperon-nucleon-nucleon forces*, *Phys. Rev. Lett.* **134**, 072502 (2025).

[78] D. Logoteta, I. Vidana, I. Bombaci, *Impact of chiral hyperonic three-body forces on neutron stars*, *Eur. Phys. J. A* **55**, 207 (2019).

[79] M. M. Nagels, Th. A. Rijken, Y. Yamamoto, *Extended-soft-core baryon-baryon model ESC16. II. Hyperon-nucleon interactions*, *Phys. Rev. C* **99**, 044003 (2019).

[80] P. Bydžovský, D. Denisova, D. Petrellis, D. Skoupil, P. Veselý, G. De Gregorio, F. Knapp, N. Lo Iudice, *Self-consistent many-body approach to the electroproduction of hypernuclei*, *Phys. Rev. C* **108**, 024615 (2023).

[81] F. Pederiva, F. Catalano, D. Lonardoni, A. Lovato, S. Gandolfi, *New insights on the hyperon puzzle from quantum Monte Carlo calculations*, arXiv:1506.04042 [nucl-th] (2015) .

[82] E. Friedman, A. Gal, ΛNN *input to neutron stars from hypernuclear data*, arXiv:2411.11751 [nucl-th] (2024).

[83] T. Gogami *et al.*, *Accurate* Λ *hypernuclear spectroscopy with electromagnetic probe at Jefferson Lab*, *AIP Conf. Proc.* **2319**, 080019 (2021).

PoS(QCHSC24)230